

Precise Thermometry for Next Generation LHC Superconducting Magnet Prototypes

V. Datskov¹, G. Kirby¹, L. Bottura¹, J.C. Perez¹, F. Borgnolutti¹, B. Jenninger¹, P. Ryan²

Abstract—The next generation of LHC superconducting magnets is very challenging and must operate in harsh conditions: high radiation doses in a range between 10 and 50 MGy, high voltage environment of 1 to 5 kV during the quench, dynamic high magnetic field up to 12 T, dynamic temperature range 1.8 K to 300 K in 0.6 sec. For magnet performance and long term reliability it is important to study dynamic thermal effects, such as the heat flux through the magnet structure, or measuring hot spot in conductors during a magnet quench with high sampling rates above 200 Hz. Available on the market cryogenic temperature sensors comparison is given. An analytical model for special electrically insulating thermal anchor (Kapton pad) with high voltage insulation is described. A set of instrumentation is proposed for fast monitoring of thermal processes during normal operation, quenches and failure situations. This paper presents the technology applicable for mounting temperature sensors on high voltage superconducting (SC) cables. The temperature measurements of fast heat cross-propagation in MQXC SC cable and FCM dynamic tests are also presented. Novel thermometry has been successfully applied to a few CERN magnet prototypes (MQXC, FCM and FRESCA2).

Index Terms — Electric resistance, Quench heaters, Temperature measurement, Superconducting coils.

I. INTRODUCTION

The conception of new superconducting magnets with record parameters requires the use of composite materials, metal alloys and superconductors with extreme mechanical and radiation characteristics. Studying the behavior of such systems at cryogenic temperature require a qualitatively new approach in the development and use of diagnostic systems, including cryogenic thermometry. During magnet quench the coils are at high voltage and experiencing rapid temperature change. Our accurate and fast thermometry can be realized by mounting the thermometer directly on zone to be measured – in our case on the SC cable. New fixation of fast cryogenic thermometer was realized by use of thin-film thermal anchor that may be glued or soldered at the desired position. To optimize thermal performance and electrical insulation of this anchor an analytical model was developed. Polyimide film meets the 50 MGy radiation requirements. Twisted manganin wires and DC measuring current of 10-30 μ A were chosen to reduce the parasitic heat load via wires and temperature sensor self-heating. Wires insulated with polyimide were tested at 4.5 K – 1.8 K and 1.5 kV. High speed recording (>200 Hz) was provided with data acquisition system MX840A [1].

Manuscript received 14th July, 2013. ¹V. Datskov¹, G. Kirby¹, L. Bottura¹, J.C. Perez¹, F. Borgnolutti¹, B. Jenninger¹, are with CERN, 1211, Geneva 23, Switzerland, (e-mail: vladimir.ivanovich.datskov@cern.ch), phone +41 22 767 1980, fax +41 22 767 6300, P. Ryan² is with Temati, Tackley, Oxford, OX5 3BL, UK.

A variety of high-voltage thin film thermal anchors and fast temperature sensor are the basis of this thermometry. In this paper we discuss its application to three magnets, recently developed at CERN: MQXC, FCM and FRESCA2. The MQXC model Quadruple of 1.8 m long has been developed at CERN for LHC accelerator insertion upgrade -Phase 1 [2-3]. The magnet incorporates several novel concepts to extract high levels of heat flux into liquid helium at 1.8 K. Internal thermometry (Fig.1) has to survive high mechanical stresses, 0-12 T fast changing magnetic field and to measure magnet rapidly rising hot spot temperatures.

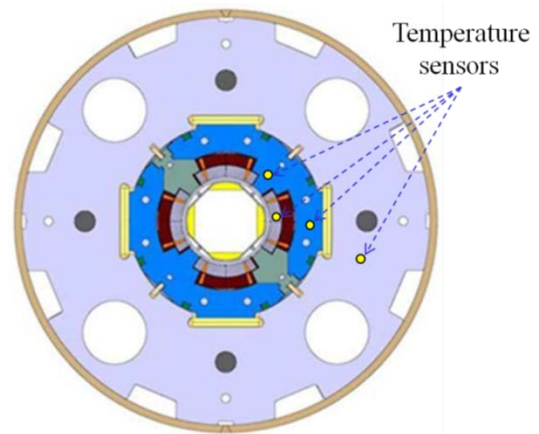


Fig. 1: MQXC magnet cross section.

Fast Cycled superconducting Magnets (FCM) is a dipole for CERN accelerator booster PS2 upgrade [4-5]. FCM dipole produces the rapid field required by the PS2 (1.8 T, 1.5 T/s). Magnet coils operate in vacuum and are made from tubular Nb-Ti cable with circulating supercritical helium flow. The internal thermometry in vacuum conditions has to measure the temperature of SC cables at voltage of 1 kV, joints and other points in the magnet structure. FRESCA2 is a 100 mm aperture Nb₃Sn dipole magnet, generating a bore field of 13 T [6-7]. It has a massive 10 tons support structure to withstand forces between coils. Thermometry was designed to control magnet cooling and to keep allowable temperature gradients.

II. CRYOGENIC TEMPERATURE SENSORS

The main objective for accelerator cryogenic thermometry is to have a precise and fast temperature measurement over a large temperature interval, for periods lasting 10 years or longer and at reasonable cost. Cryogenic sensor suppliers do not offer a warranty on qualitative thermometry for 10-15 years. Therefore in-house development of thermometry application for magnets are required to make it cheaper, reliable and satisfying the challenging specifications. The

LHC accelerator calibration group at CERN in 1998 has conducted the irradiation tests of seven selected resistive-type temperature sensors at cryogenic conditions [8]. Three types of cryogenic sensors have been selected for applications able to withstand the radiation conditions of LHC accelerator. After being irradiated with a neutrons dose of 4×10^{14} n/cm² at 1.8 K, a temperature shift of +2 mK was observed for the AB (Allan Bradley) carbon sensors, shift of +0.3 mK for Carbon Ceramic Sensor (CCS-Russian name is TVO) [9] and shift of +1 mK for CX (Cernox) [10] sensor. After neutron dose of 1.1×10^{17} n/cm² TVO sensor had a shift of 0.04 K at 4.2 K [11]. AB and CCS sensors response time is 8 ms and 1 ms at 4.2 K accordingly [12]. Comparison [13] showed that on the market there are two cryogenic temperature sensors CX [10] and CCS [14] which have similar electrical characteristics. The major parameters of these sensors are presented in the Table I. CCS sensors offer a good long-term stability and fast response due to silver-leads diffuse electrical contacts and ceramic body.

Table I.
COMPARISON OF TEMPERATURE SENSORS

Sensor type	Price/each from company	Resistance at: 300 K/4.2 K Ω	Long-term stability at 4.2 K	Time response at 4.2 K
CX-1050	665 USD	60/3500	25 mK/year	15 ms
CCS/A	380 USD	920/3500	1 mK/year	1 ms

III. THERMAL ANCHOR DESIGN

The thermal anchors that are used in our setup are based on the commercially available polyimide (Kapton) film with thin metallic layers (generally gold plated copper) on either side. On one side metallic strips are prepared by lithography or chemical etching. The electrical wire is soldered on one side of the strip whereas the lead of the temperature sensor is soldered at the opposite end. The substrate (0 in Fig. 2) is at the temperature T_0 , which is the quantity we want to measure. The heat Q_b from the wire as a result of thermal conductance is evacuated along the strip, resulting in a remaining temperature T_c where the temperature lead is connected. Depending on the material choice and dimensions, the thermal anchor can be optimized such that the difference between T_c and the temperature T_0 to be measured is minimized.

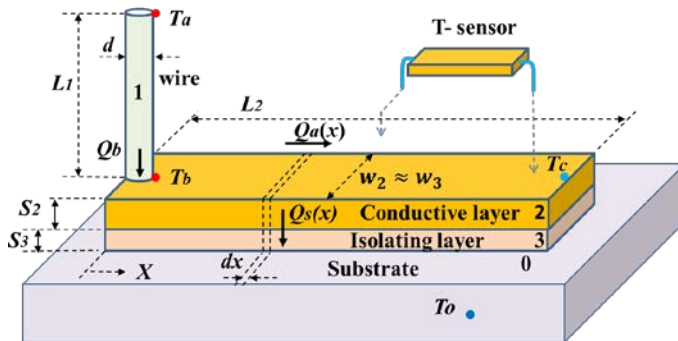


Fig. 2: Schematic of a thermal anchor based on metal strips on a polyimide film: 0 - substrate, 1 - wire, 2 - conductive layer, 3 - polyimide insulator layer.

The following equations are an analytical approach to estimate this difference. Symbols description for equations below are as the following: k -thermal conductivity, L -length, s -thickness, A -cross-section, w -width of wire and layers, T_a and T_b -wire temperature, T_c -conductive layer temperature, Q_a -heat flux along thermal anchor (function of x), Q_b - heat flux from connecting wire. The conductive heat load along the wire is:

$$Q_b = \frac{A_1}{L_1} \int_{T_a}^{T_b} k_1 dT \quad (1)$$

The heat flux across the thermal anchor causes the variation of the heat flux along the thermal anchor.

$$\frac{dQ_a}{dx} = -\frac{w_3}{s_3} \bar{k}_3 \Delta T(x) \text{ with } \Delta T(x) = T_2(x) - T_0 \quad (2)$$

The heat flux along the thermal anchor is:

$$Q_a(x) = -w_2 s_2 k_2 \frac{dT_2}{dx} \quad (3)$$

Differentiation gives and applying the definition $\Delta T(x)$:

$$\frac{dQ_a}{dx} = -w_2 s_2 k_2 \frac{d^2 \Delta T(x)}{dx^2} \quad (4)$$

Equation 2 with equation 4 gives:

$$-\frac{w_3}{s_3} \bar{k}_3 \Delta T(x) = -w_2 s_2 k_2 \frac{d^2 \Delta T(x)}{dx^2} \quad (5)$$

By defining $\alpha = \frac{k_3}{s_3 s_2 k_2}$ and $w_2 \approx w_3$, as well as considering the thermal conductance being constant in the temperature range (hence using their mean values), the corresponding differential equation is:

$$\Delta T'' - \alpha \Delta T = 0 \quad (6)$$

With the boundary conditions:

$$Q_a(x=0) = Q_b \text{ and } Q_a(x=L_2) = 0 \quad (7, 8)$$

And the following definitions:

$$\psi = \frac{Q_0}{\sqrt{\alpha} w_2 s_2 k_2} \text{ and } \rho = \frac{e^{-\sqrt{\alpha} L_2}}{2 \sinh(\sqrt{\alpha} L_2)} \quad (9, 10)$$

The following solution to the upper differential equation can be found as the following:

$$\Delta T(x) = \psi(e^{-\sqrt{\alpha} x} + 2\rho \cosh(\sqrt{\alpha} x)) \quad (11)$$

Figure 3 shows the calculated temperature gradient along a thermal anchor based on equation (11).

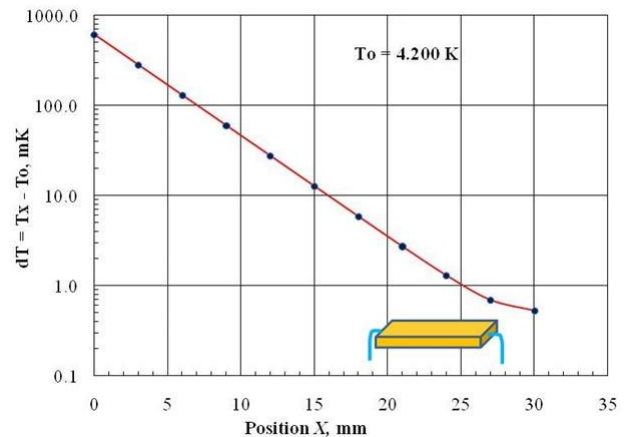


Fig. 3: Calculated temperature gradient along the strip.

In this calculation the copper strip size was $1.6 \times 30 \times 0.018$ mm, and we had a 0.05 mm thick polyimide foil. For copper we used the mean thermal conductance 500 W/m/K, and for polyimide 0.3 W/m/K. In vacuum the heat load from 300 K to 4.2 K via copper electrical wire with diameter of 0.1 mm and length of 0.5 m is about 2.3 mW. As shown on the graph, the error in the measurement even in this unfavorable situation

with copper wires would still be below 1mK. Such thermal anchor have been named “thermal pad” and is commercially available [14]. Some later research has demonstrated their reliability in applications including: compatibility with UHV systems, a good electrical insulation (polyimide coated strips tested up to 1.5 kV), and no property change after soldering on the desired metal surface. To improve electrical insulation voltage it would be necessary to increase the gap between copper strips on the surface of the thermal anchor.

IV. THERMOMETRY APPLICATION

A. MQXC thermometry

For the MQXC model we developed a test rig to characterize fast performance of CCS sensors. Two CCS sensors were mounted with thermal pads, which were glued on two sides of MQXC flat SC cable using VGE-7031 varnish [10]. The goal of the test was checking of the heat transfer and the time response of sensors during the fast pulse heating of MQXC SC cable, immersed in liquid helium. The fast heat pulse was done by discharging of 10 mF capacitor (0-80V) into a spot heater, glued on one side of SC cable. Sensor T1 was mounted on the surface of spot heater and another T2 was mounted on the opposite side of SC cable (Fig. 4).



Fig. 4: CCS sensor T2, mounted on MQXC superconducting cable with use of thermal pad.

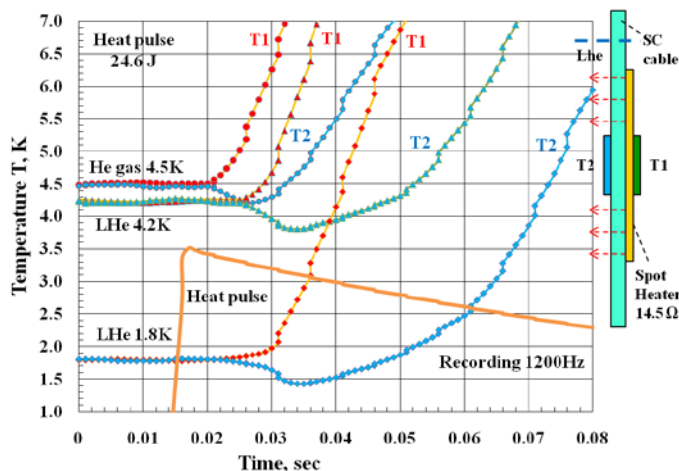


Fig. 5: MQXC spot heater cryogenic testing.

From recorded data at rate of 1200 Hz one can deduce (Fig. 5) a fast time response of T1 sensor on the spot heater in the

range of 3-5 ms in helium gas at 4.5 K. The presence of liquid helium delays the response time up to 8-10 ms. Other sensor T2 showed temperature dropping during 10-20 ms. Using modified thermal pads geometry it was possible to mount CCS sensors on several locations of MQXC magnet coils (Fig. 6-7).

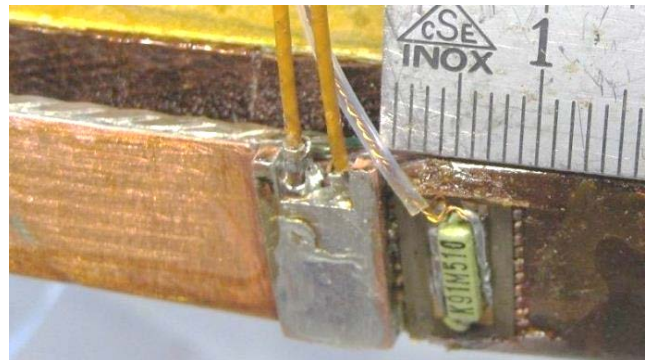


Fig. 6: CCS sensor and thermal pad, mounted on MQXC coil conductor near voltage taps.

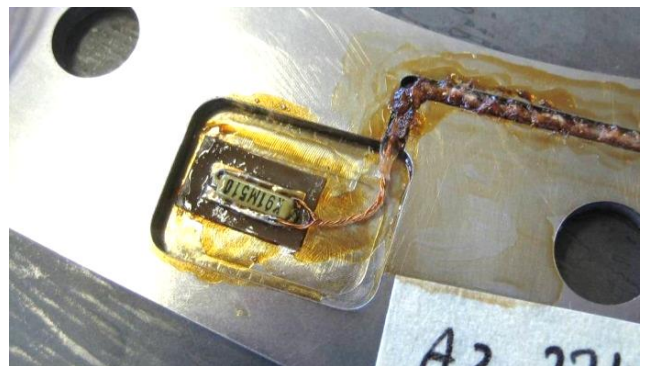


Fig. 7: CCS sensors and thermal pads, mounted on MQXC lamination.

B. FCM thermometry

FCM magnet with tubular SC cable in vacuum had a strict requirement for cryogenic temperature sensors, which include the following: mounting of sensors on a round surface of SC cable with electrical insulation of 1 kV to the cable, accuracy of measurements better than 0.01 K in the temperature range of 4-20 K during the fast current ramping in the magnet.

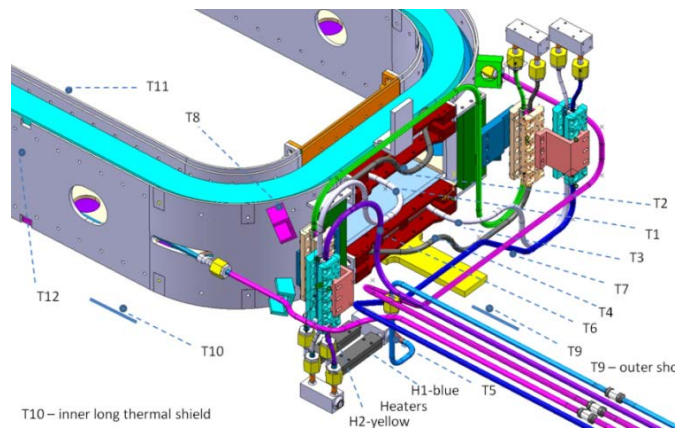


Fig. 8: CCS sensors allocation in FCM magnet.

Twelve CCS sensors were mounted in different locations of FCM magnet (Fig. 8) using glued straight and soldered curved thermal pads (Fig. 9). During calorimetric measurement we

increased the heating in steps of 5-10-15-20 W of helium flow with the heater mounted on the helium supply pipe >1 m before the inlet of FCM coils.

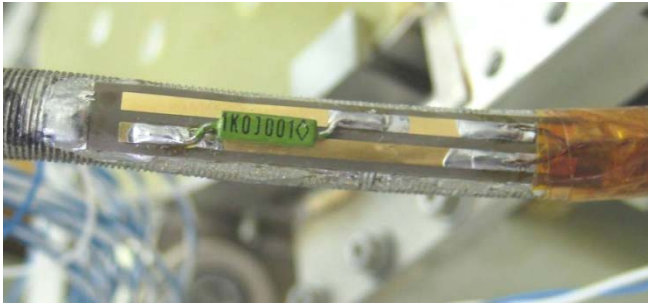


Fig. 9: Curved thermal pad with CCS sensor on FCM cable.

Recorded data has shown a 2 s time response of T3 sensor on the second coil inlet (Fig. 10).

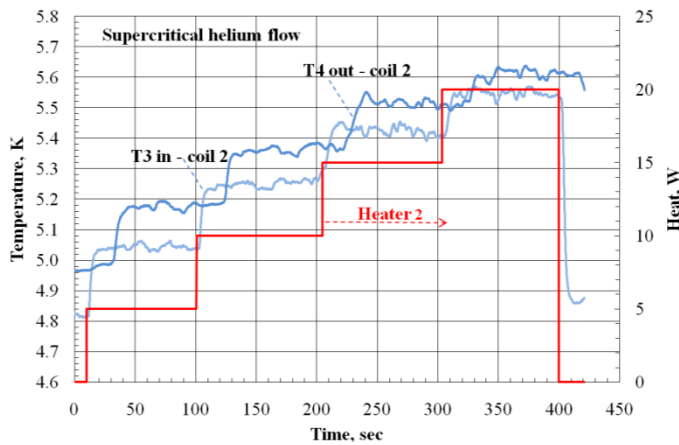


Fig. 10: FCM coil 2 heating during calorimetric test.

C. FRESCA2 thermometry

FRESCA2 magnet requires a special technology of sensors mounting in holes of massive magnet support components using metal screws of different size. All components of this magnet are immersed in cryogenic liquid: during cool-down in liquid nitrogen and in liquid helium at working conditions. Accurate cryogenic thermometry in massive metal structure immersed in cryogenic liquid is not trivial. One has to ensure a

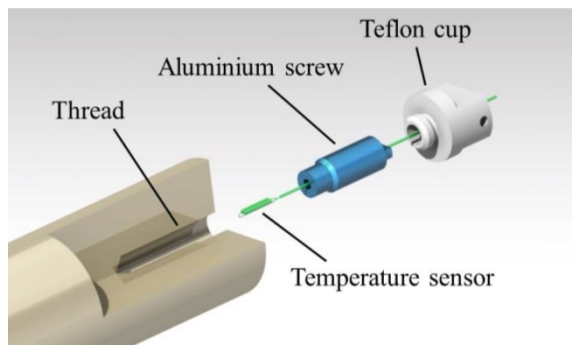


Fig. 11: FRESCA2 temperature sensor in the screw.

good thermal contact of thermometer to the metal body and fixture seal from cryogenic liquid. Magnet support is made of Al-alloy and sensor mounting technique was chosen with the

use of aluminum screws and Teflon screw-cups (Fig. 11). To examine the performance of FRESCA2 thermometry a special test rig was created. In the top and bottom of aluminum alloy cylinder two CCS sensors were mounted with screws size M10. The edge of the screw with mounted sensor had a good thermal contact inside of aluminum body using Apiezon-N grease [10]. The cool-down in liquid nitrogen showed smooth temperature T1 decreasing at the bottom (Fig.12). This confirms no liquid nitrogen has penetrated to the sensor. A batch of 10 CCS sensors, mounted as Fig. 11 in the dummy magnet system. Cool-down of this 10 tons system till 77.4 K over 1 week demonstrated that temperature gradients were within the allowed range.

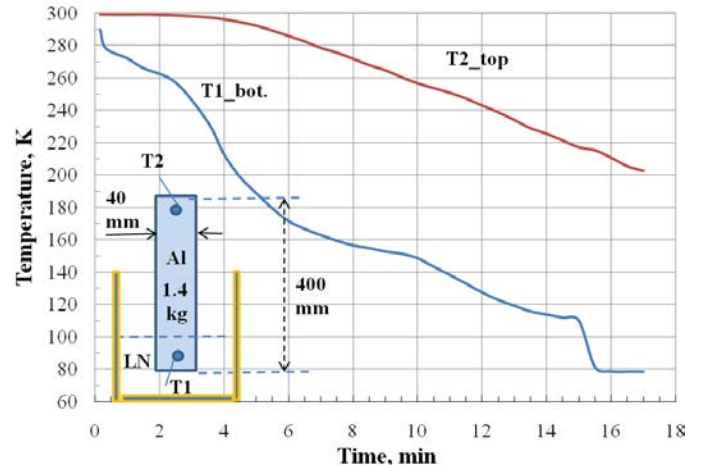


Fig. 12: FRESCA2 model cylinder cooling in liquid nitrogen.

V. CONCLUSION

Precise thermometry, based on thin-film thermal pads and fast, low cost CCS carbon-ceramic sensor, performed well during the cryogenic tests of three CERN projects: MQXC, FCM and FRESCA2. Different mounting techniques of CCS sensors were applied in each system. With this thermometry we could record the pulsed heat propagation from the MQXC spot heater through SC cable. The time response of CCS sensor mounting fixture was in the range 3-5 ms at 4.5 K in helium gas. This system permits the future studies of high heat fluxes with high voltages through the equipment needed for the Hi-Luminosity LHC upgrade foreseen in 2022.

ACKNOWLEDGMENT

The authors thank the teams in CERN MSC group, Cryo-Lab, and SM18 for their help with assembling and testing of the selection of sensor set-up's. In particular: Laetitia Dufay-Chanat for help with cryogenic insert, Michael Guinchard for guidance and the implementation of the fast data acquisition system, Vincent Roger for analysis of FCM data.

REFERENCES

- [1] <http://www.hbm.com/en/menu/products/measurement-electronics-software/compact-universal-data-acquisition-system/quantumx-mx840a/>
- [2] G.A. Kirby *et al.* "Engineering Design and Manufacturing Challenges for a Wide-Aperture, Superconducting Quadrupole Magnet", *IEEE Trans. Magn.*, 22 (2012).
- [3] G. Kirby *et al.* " LHC IR Upgrade Nb-Ti, 120mm Aperture Model

- Quadrupole Test Results at 1.8 K”, Presentation 3OrCC-04, MT23.
- [4] L. Bottura *et al.* “The Fast Cycled superconducting Magnets (FCM) R&D program at CERN”, HHH-2008 proceedings, pp. 71-75.
 - [5] G. Willering *et al.* “Fast Cycled Magnet (FCM) demonstrator program at CERN: Test station, instrumentation and measurement campaign”, Presentation 4OrCB-05, MT23.
 - [6] P. Ferracin *et al.*, “Development of the EuCARD Nb3Sn Dipole Magnet FRESCA2”, *IEEE Trans. Magn.*, 23 (2013).
 - [7] J.E. Muñoz Garcia *et al.* “Assembly, loading, and cool-down of the FRESCA2 support structure”, Presentation 3PoAF, MT23.
 - [8] J-F. Amand *et al.*, “Neutron Irradiation Tests in Superfluid Helium of LHC Cryogenic Thermometers”, CERN-LHC Project report #209, July 1998.
 - [9] V.I. Datskov and J.G. Weisend II, “Characteristics of Russian Carbon Resistance (TVO) Cryogenic Thermometers”, ICEC-15 Proceedings, Cryogenics. 1994, Vol.34, pp. 425-428.
 - [10] <http://www.lakeshore.com/products/Cryogenic-Temperature-Sensors/Cernox/>
 - [11] V. Datskov *et al.*, “Long-life cryogenic thermometry in particle accelerators and other demanding applications”, *IEEE Trans. Magn.*, 10 (2000), pp.1403-1406.
 - [12] V.I. Datskov *et al.*, “Inertial characteristics of cryogenic temperature sensors”, Preprint of JINR, 8-83-45, Dubna, 1983, (in russian).
 - [13] Süßer M., “Comparison of TVO – and Cernox temperature sensors”, Proceedings of ICEC 22-ICMC 2008, pp. 479-482
 - [14] <http://www.temati-uk.com/>